



# THE STRUCTURE OF AMORPHOUS PHOSPHORUS

S. Elliott, J. Dore, E. Marseglia

## ► To cite this version:

S. Elliott, J. Dore, E. Marseglia. THE STRUCTURE OF AMORPHOUS PHOSPHORUS. Journal de Physique Colloques, 1985, 46 (C8), pp.C8-349-C8-353. 10.1051/jphyscol:1985852 . jpa-00225195

**HAL Id: jpa-00225195**

**<https://hal.science/jpa-00225195>**

Submitted on 4 Feb 2008

**HAL** is a multi-disciplinary open access archive for the deposit and dissemination of scientific research documents, whether they are published or not. The documents may come from teaching and research institutions in France or abroad, or from public or private research centers.

L'archive ouverte pluridisciplinaire **HAL**, est destinée au dépôt et à la diffusion de documents scientifiques de niveau recherche, publiés ou non, émanant des établissements d'enseignement et de recherche français ou étrangers, des laboratoires publics ou privés.

## THE STRUCTURE OF AMORPHOUS PHOSPHORUS

S.R. Elliott, J.C. Dore<sup>+</sup> and E. Marseglia<sup>++</sup>*Department of Physical Chemistry, University of Cambridge, Lensfield Road, Cambridge, U.K.**<sup>+</sup>Department of Physics, University of Kent, Canterbury, U.K.**<sup>++</sup>Cavendish Laboratory, University of Cambridge, Madingley Road, Cambridge, U.K.*

**Résumé** - La structure du phosphore rouge amorphe a été étudiée en diffraction neutronique, sur un réacteur statique et une source de neutrons pulsée. Les fonctions de corrélation dans l'espace réel, obtenues par transformée de Fourier des données expérimentales, ont été comparées avec les résultats de calculs pour un réseau continu aléatoire triplement coordonné, relaxé dans un mélange de potentiels interatomiques liants et antiliants. L'accord entre la théorie et l'expérience est assez limité. Ceci est attribué à la présence de différents types d'ordres intermédiaires dans le solide amorphe, comme par exemple la formation d'amas de type cage qui sont caractéristiques de la forme monoclinique (Hittorf) du phosphore.

**Abstract** - The structure of amorphous red phosphorus has been studied by neutron diffraction, using both reactor and pulsed neutron sources. Real-space pair correlation functions obtained by Fourier transformation of the experimental scattering data have been compared with those calculated for a three-fold coordinated CRN model, which had been energy-relaxed using a combination of bonding and non-bonding interatomic potentials. Only moderate agreement between theory and experiment was found. The discrepancies are ascribed to the presence of a considerable degree of intermediate-range order in the amorphous solid, in particular consisting of cage-like clusters characteristic of the monoclinic (Hittorf) form of phosphorus.

## I - INTRODUCTION

The determination of the structure of amorphous solids using conventional diffraction experiments alone is in general difficult because interpretation of the scattering data is not straightforward, particularly for multicomponent amorphous systems, where the measured scattering intensity is a suitably weighted sum of contributions from the various types of interatomic correlations. Obviously, the problem is simplest for an elemental material where the maximum amount of structural information can be inferred from a single scattering experiment.

This paper reports the results of a neutron-scattering study of elemental amorphous red phosphorus, which is a material whose structure is of interest in view of the wide variety of crystalline polymorphs which occur. In particular, the question at issue is to what extent does the intermediate-range order in the amorphous solid (if any) reflect structural arrangements characteristic of particular crystalline polymorphs.

Phosphorus in its various crystalline polymorphs is invariably three-fold coordinated, but a variety of structural conformations can occur [1]: white P is a molecular solid consisting of aggregates of  $P_4$  molecules which are Van-der-Waals bonded together; rhombohedral black P is a sheet structure consisting of single layers of atoms comprised of identical 6-fold rings in which each atom adopts a "staggered" configuration (with a dihedral angle,  $\phi = 180^\circ$ ); the more common orthorhombic form of black P is again a layered structure having double layers consisting of identical 6-fold rings in which only two of the bonds are staggered, the rest having a "semi-staggered" configuration ( $\phi = 70^\circ$ ); violet P, the monoclinic (Hittorf) form, is again a layer structure, but is considerably more complicated with the basic structural unit consisting of cage-like  $P_8$  and  $P_9$  clusters connected together alternately,

thereby forming tubes of pentagonal cross-section which are themselves held together by Van der Waals' forces to form layers. This structure has both eclipsed ( $\phi = 0^\circ$ ) and semi-staggered ( $\phi = 70^\circ$ ) configurations, but no staggered bonds.

## II - EXPERIMENTAL

Samples of bulk red a-P, made by thermal conversion from white P /2/, were used in this study. Measurements were taken using both reactor and pulsed neutron sources. The former utilized the D4 diffractometer at the ILL, using neutrons with wavelength  $\lambda = 0.69\text{\AA}$ , and also the Curran diffractometer on the Dido reactor at AERE, Harwell using  $\lambda = 1.37\text{\AA}$  neutrons. The pulsed neutron measurements, made using the TSS Mk.II spectrometer at the Helios electron linac, AERE, Harwell, enabled the scattering data to be extended to high values of  $Q$  ( $\approx 30\text{\AA}^{-1}$ ); all the data sets were combined to give the total scattering intensity,  $I(Q)$ , shown in Fig. 1. Further details of data collection and analysis are given elsewhere (Dore, Steytler, Marseglia and Elliott, to be published).

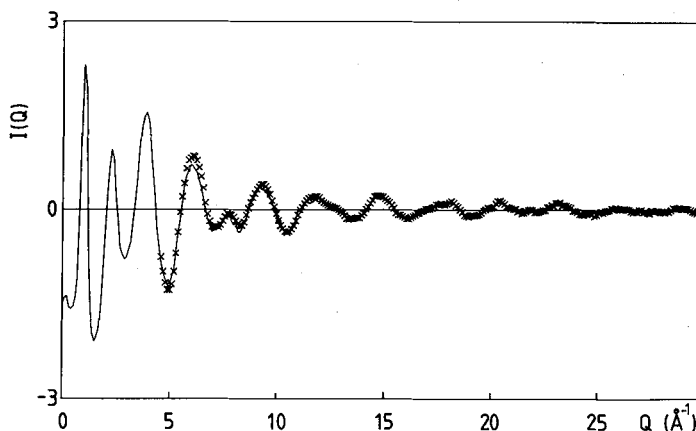


Fig. 1 - Scattering intensity of a-P measured using both reactor and pulsed neutron sources.

## III - EXPERIMENTAL RESULTS

Fourier transformation of the function  $QI(Q)$  yielded the reduced RDF,  $G(r)$ , shown in Fig. 2. Two sharp peaks are evident at 2.224 and 3.49 $\text{\AA}$ , followed by a series of subsidiary peaks at higher values of  $r$ . The first two coordination shells lying at  $r_1$  and  $r_2$  are reasonably well-defined, and the position and width of the second peak relative to the first therefore allows an estimate of the average bond angle and its RMS variation to be made; a value of  $\theta = 103.4 \pm 7.6^\circ$  is thereby obtained. An estimate of the nearest-neighbour coordination number can be obtained from the area under the first peak in the RDF,  $(J(r) = rG(r) + 4\pi r^2 \rho_0)$  where  $\rho_0$  is the average macroscopic density). Owing to normalization difficulties due to the irregularly shaped sample, a precise value of the coordination number is somewhat uncertain; scaling the  $G(r)$  curve such that the density, obtained from the straight line region below the first peak where  $G(r) = -4\pi r \rho_0$ , equalled the literature value for the density,  $\rho_0 = 2.09 \text{ g cm}^{-3}$ , gave a coordination number of  $N_1 = 3.2 \pm 0.05$ . The RDF resulting from this procedure is shown in Fig. 3. Whilst being reasonably consistent with 3-fold coordination, this procedure for obtaining  $N_1$  is subject to error if the material contains voids, as is known to be the case from SEM studies /3/; if  $N_1$  is set equal to 3, the inferred density then becomes  $\rho_0 = 1.95 \text{ g cm}^{-3}$ . The values for the various short-range structural parameters obtained in this study are

are in good agreement with those found in a previous X-ray diffraction study of red a-P /4/, namely  $r_1 = 2.24\text{\AA}$ ,  $r_2 = 3.48\text{\AA}$ ,  $\theta = 101.9^\circ$ ,  $N_1 = 2.97$ . For comparison, the RDF obtained from the X-ray diffraction study /4/ is also shown in Fig. 3.

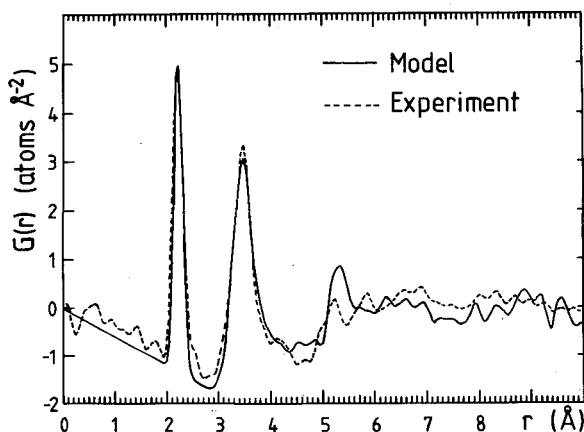


Fig.2. Reduced RDF obtained from the neutron scattering intensity of Fig. 1 compared with that calculated for a CRN model (see text for details).

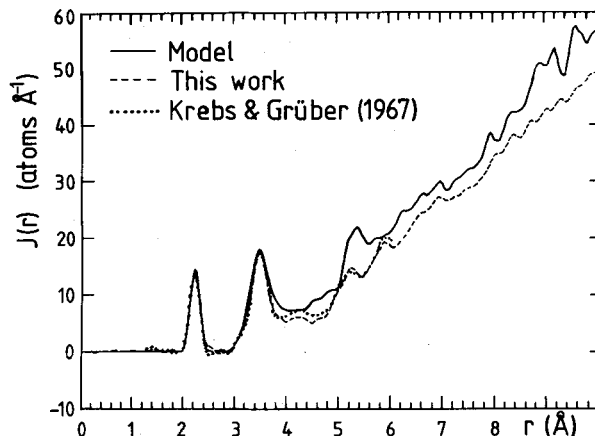


Fig. 3. RDF obtained from the present neutron scattering data compared with earlier X-ray data /4/ and the RDF calculated for a CRN model.

Detailed examination of the shape of the second peak in the RDF shows it to be different from that of the first and a considerable distortion from a gaussian line-shape is found; it is broader at the base, particularly on the low- $r$  side. Such a shape could result from an asymmetric bond-angle distribution,  $P(\theta)$ , or even a bi-modal  $P(\theta)$  with the main contribution lying at the average bond angle,  $\theta = 103^\circ$ , with a lesser contribution at a smaller angle,  $\theta \approx 95^\circ$ . This point, and a consideration of the peaks in the RDF lying beyond the second shell, will be discussed later.

#### IV - MODELLING STUDIES

In order to be able to interpret further the experimental results, a structural model

of a-P was constructed. A 3-fold coordinated "ball-and-stick" continuous random network (CRN) model, originally constructed to simulate the structure of a-As /5,6/, was used as a starting point, and the model was modified by computer means to alter the average bond angle to the value characteristic of a-P, whilst leaving the topology (ring statistics etc.) unchanged. The modification was effected by subjecting the "atoms" in the model to an energy relaxation procedure in which both bonding interactions (Keating potential for bond stretching and bending /7/) and non-bonding interactions (Buckingham or exp-6 potential /8/) were used; details of the relaxation procedure are given elsewhere (Elliott, Carter, Marseglia and Dore, to be published).

The RDF of the energy-relaxed model was calculated from the atomic coordinates, corrected for the finite size of the model, and the resulting RDF in histogram form was then convoluted with a gaussian to simulate both thermal and instrumental broadening effects. Although such a broadening procedure is insufficient to permit a detailed study of the peak *shapes*, only a qualitative comparison of the calculated curves is attempted here, and so such a limitation is of little account.

The calculated reduced RDF,  $G(r)$ , for the model is compared with the experimental neutron data in Fig. 2, and the calculated RDF,  $J(r)$ , is compared with both the present neutron and earlier X-ray /4/ results in Fig. 3. It can be seen that there is good agreement between the model and experimental curves for the first two peaks. This, however, is not too surprising, since the model has 3-fold nearest-neighbour coordination and the bond length is scaled to the experimental value. Furthermore, the average bond angle is set to the experimental value in the energy relaxation program, and so the position of the second peak is expected to match experiment.

#### V - DISCUSSION

Considerable discrepancies between the model and experiment occur, however, at larger distances. The most obvious difference is in the average density; as can be seen from Fig. 3, the model has a density 15-20% higher than experimentally observed values. Varying the parameters in the interatomic potentials, in particular the relative strength of bonding and non-bonding interactions, gave at most only a 1% change in density. The discrepancy must therefore be ascribed to a failing of the model. The CRN model, as built, contains oblate voids which are a consequence of the 2D geometry characteristic of  $p^3$  bonding /6/. Red a-P prepared from white P /2/ has a spherulite growth morphology /3/, and as a consequence would have a higher void concentration, and therefore lower density, than an otherwise homogeneous material. Although this may be one reason for the discrepancy in density, another reason may have to do with intermediate-range order (IRO). The CRN model contains no intentional IRO, i.e. particular ring sizes or clusters etc.; if such forms of IRO were actually present in the real material, packing constraints would probably ensure a lower overall density than for an amorphous structure not containing such large, well-defined structural arrangements.

A further striking difference between the model RDF and experiment is in the relative size and position of the third peak; the model peak is much larger in height, and lies at a larger distance, than is found experimentally (see Fig. 2). The principal contribution to the third peak at  $r_3 = 5.3\text{\AA}$  comes from 3-bond correlations in semi-staggered or staggered conformations (with a relative frequency of occurrence of 1:2); eclipsed configurations give 3-bond correlations at 2.85 and 4.4\AA. The CRN model used in this study does not have a random dihedral-angle distribution, but staggered configurations are approximately twice as probable as eclipsed configurations /6/. From this, we may infer that a-P contains a much higher proportion of non-staggered, probably eclipsed, configurations than is present in the CRN model.

A similar conclusion can be reached from a consideration of the small features observed experimentally between the second and third peaks in the RDF. A random dihedral-angle distribution would give rise to a featureless minimum in this region, and so the observation of features in the RDF at such distances immediately suggests the existence of preferred conformations, and hence values of  $\phi$ , in a-P. In

particular, the peak lying at  $4.8\text{\AA}$  can only arise from *eclipsed* configurations having large ( $\theta \sim 103^\circ$ ) bond angles. The other prominent peak at  $4.3\text{\AA}$  can be ascribed either to eclipsed configurations with smaller ( $\theta \sim 96^\circ$ ) bond angles, or to semi-staggered configurations containing a mixture of large and small bond angles in which  $\phi$  is determined by the smaller bond angle.

Thus, it appears that the features in the RDF of a-P lying in the range  $4\text{--}6\text{\AA}$  arise from a preponderance of eclipsed and/or semi-staggered configurations. It should be noted that *eclipsed* configurations do *not* occur in the orthorhombic black P structure, and so the suggestion /4,9/ that the IRO in a-P is characteristic of this polymorph is therefore unlikely to be true. It is interesting to note, however, that both eclipsed and semi-staggered (but not staggered) configurations occur in the Hittorf monoclinic form, which consists of  $P_8$  and  $P_9$  clusters. We suggest that, on the basis of the diffraction evidence, the IRO in a-P is characteristic of Hittorf's P, namely that  $P_8$  (and perhaps  $P_9$ ) clusters exist in the structure.  $P_8$  units, in particular, can readily form by polymerization of two  $P_4$  molecules in the white P precursor, with minimal atomic movement. Confirmatory evidence for the presence of  $P_8$  or  $P_9$  clusters comes also from an analysis of the Raman spectrum of a-P /10/.

## VI - CONCLUSIONS

A high-resolution neutron scattering study of red a-P has been performed. Comparison of the experimental RDF with that of a CRN model having minimal intermediate-range order (IRO) reveals substantial discrepancies in the region of the third and fourth peaks. It is suggested that the IRO in a-P is similar to that found in the Hittorf, monoclinic form of P, namely  $P_8$  (or  $P_9$ ) clusters are present.

## ACKNOWLEDGEMENTS.

We are grateful to Drs. D.C. Steytler, P. Chieux and E.K. Osae for assistance with the diffraction experiments and to Mr. R.D. Carter for assistance with the structural modelling.

## REFERENCES

- /1/ Corbridge, D.E.C., "The Structural Chemistry of Phosphorus" (Elsevier : 1974).
- /2/ a-P samples obtained from Mining and Chemical Products Ltd, Alpertons, Wembley, U.K.
- /3/ Extnance, P. and Elliott, S.R., Phil. Mag. B43 (1981) 469.
- /4/ Krebs, H. and Grüber, H.U., Z. Naturforschg. 22(a) (1967) 96.
- /5/ Greaves, G.N. and Davis, E.A., Phil. Mag. 29 (1974) 1201.
- /6/ Greaves, G.N., Elliott, S.R. and Davis, E.A., Adv. Phys. 28 (1979) 149.
- /7/ Keating, P.N., Phys. Rev. 145 (1966) 637.
- /8/ Maitland, G.C., Rigby, M., Smith, E.B. and Wakeham, W.A. "Intermolecular Forces" (Clarendon Press : 1981).
- /9/ Beyeler, H-U and Veprek, S., Phil. Mag. B41 (1980) 327.
- /10/ Fasol, G., Cardona, M., Hönle, W. and Von Schnering, H.G., Sol. St. Comm. 52 (1984) 307.